Morphological and Dose-Dependent Study on the Effect of Methyl, Hexyl, and Dodecyl Rosmarinate on Staphylococcus carnosus LTH1502: Use of the Weibull Model

Sarisa Suriyarak, Herbert Schmidt, Pierre Villeneuve, Jochen Weiss

Journal of Food Protection, Vol. 81, No. 4, 2018, Pages 598–605
doi:10.4315/0362-028X.JFP-17-334

Research Paper

Morphological and Dose-Dependent Study on the Effect of Methyl, Hexyl, and Dodecyl Rosmarinate on *Staphylococcus carnosus* LTH1502: Use of the Weibull Model

SARISA SURIYARAK,[1,2]* HERBERT SCHMIDT,[3] PIERRE VILLENEUVE,[4] AND JOCHEN WEISS[5]

[1]*Department of Food Technology, Faculty of Science, and* [2]*Emerging Process for Food Functionality Design Research Unit, Chulalongkorn University, Phayathai, 10330 Bangkok, Thailand (ORCID: http://orcid.org/0000-0003-4873-6378);* [3]*Department of Food Microbiology, Garbenstrasse 28, and* [5]*Department of Food Physics and Meat Science, Garbenstrasse 21/25, Institute of Food Science and Biotechnology, University of Hohenheim, 70599 Stuttgart, Germany; and* [4]*Centre de Coopération Internationale en Recherche Agronomique pour le Dévelopment (CIRAD), Unité Mixte de Recherche (UMR), Ingénierie des Agropolymères et Technologies Emergentes (IATE), Montpellier, 34060 France*

MS 17-334: Received 9 August 2017/Accepted 20 November 2017/Published Online 12 March 2018

ABSTRACT

The mechanisms of three antimicrobial rosmarinates (methyl-RE1, hexyl-RE6, and dodecyl-RE12) were investigated against *Staphylococcus carnosus* LTH1502. Scanning electron microscopy was used to determine the morphology of treated cells to gain information on potential changes in the site of action of compounds. The survival data obtained from antimicrobial activity assays were fitted to a nonlinear Weibull model to assess changes in inactivation behavior. Generally, esters became more effective with increasing length of the alkyl chain, resulting in a lower concentration for inhibition and inactivation. Weibull distribution parameters showed a downward concave inactivation pattern for RE1 above a critical concentration, indicative of a delayed log phase of the antimicrobial activity, with few cells being inactivated immediately after treatment and more cells being affected at later times. In contrast, esters having longer alkyl chains (RE6 and RE12) had an upward concave inactivation behavior, with more cells being inactivated immediately after addition of compounds. Cellular morphologies suggest that the antimicrobial mode of action of esters transitions from one that acts intracellularly (RE1) to one that predominately affects bacterial membrane (RE6 and RE12) due to changes in physicochemical properties of esters. Assessment that is based on the parameters of the Weibull model could, thus, be used to evaluate antimicrobial efficiency, in addition to MIC.

Key words: Antimicrobials; Esterification, Rosmarinate; *Staphylococcus carnosus*; Weibull model

Food antimicrobial agents are compounds that are commonly added to food matrices, food packaging materials, food contact surfaces, or food processing environments to inhibit the growth of, or inactivate, food pathogens or spoilage microorganism *(7)*. With the emergence of minimal processing approaches, the use of antimicrobials has become more prevalent because additional hurdles to growth are needed to ensure safety and to prolong the shelf life of foods *(22, 31)*. Therefore, there is a great interest in expanding the number of available food antimicrobial compounds.

The development or discovery of "new" food antimicrobials is, however, quite difficult because researchers have to carry out elaborate screening tests for candidate compounds to assess how they affect the growth of targeted microorganisms *(14)*. Moreover, their activity in food matrices, and not only in model microbiological media, has to be established *(7)*. Thus, rather than discovering new ones, it may be simpler to modify existing ones such that activities in model systems and foods are enhanced. This may be done by a variety of chemical reactions to alter structure and conformation of antimicrobials *(10)*. For example, amidation of lactoferrin and β-lactoglobulin with 1-ethyl-3-[3-(dimethylamino) propyl] carbodiimide increased the net positive charge of both compounds, in turn increasing their antimicrobial activity. The antimicrobial activity of conjugates formed by Maillard reaction of chitosan with xylan similarly increased activity against *Escherichia coli* and *Staphylococcus aureus (16)*. Min et al. *(23)* used a hydrolysis approach to generate flavonoids from glycosidic isoflavones to obtain compounds that were not antimicrobially active against *Bacillus cereus, S. aureus,* and *Listeria monocytogenes*. Whereas these approaches have been successful, the establishment of robust structure–function relations with predictive ability to better guide such antimicrobial modification reactions has been scarce.

In the laboratories involved in this study, initially an esterification approach was used to enhance the activity of rosmarinic acid [(*R*)-α-[[3-(3,4-dihydroxyphenyl)-1-oxo-2*E*-propenyl]oxy]-3,4-dihydroxy-benzeneproanoic acid] by reacting it with a series of alkyl alcohols under acidic conditions *(32, 33)*. Rosmarinic acid was used as a starting material because it is a natural phenolic compound *(28)* found in many plants such as rosemary (*Rosmarinus*

* Author for correspondence. Tel: +66 2218 5521; Fax: +66 2254 44314; E-mail: sarisaam@gmail.com.

officinalis), sage (*Salvia officinalis*), lemon balm (*Melissa officinalis*), and oregano (*Origanum vulgare*) *(6, 18, 27)*. It has been shown to be antimicrobially active against gram-positive organisms such as *Staphylococcus epidermidis, Stenotrophomonas maltophilia, S. aureus,* or *L. monocytogenes (1, 13, 24)*.

When the activity against a model microorganism (*Staphylococcus carnosus* LTH1502) was assessed, it was found that a chain-length–dependent activity with medium chain (C8 to C12) ester was significantly more active than those with short (<C6) or long (>C16) chains. It was suggested at the time that the esterification may have caused the compounds' affinities for microbial cells to increase and at the same time the solubility to decrease, thereby leading compounds to show first increasing, and then decreasing, activities. At the time, it was, however, not possible to fully confirm this hypothesis and to subsequently establish a working structure–function relationship.

The current study was undertaken to gain a better understanding of the changes in mode of action of rosmarinic acid esters (REs). Therefore, a more detailed dose-dependence and cellular morphology study was conducted with only select REs (methyl, hexyl, and dodecyl rosmarinate). Macrobroth dilution assays were used to obtain log CFU per milliliter versus incubation time curves, and treated cells were observed under a scanning electron microscope (SEM). Only inactivation curves of REs were analyzed with a nonlinear kinetic model to obtain parameters indicative of changes in the mode of action of compounds.

The Weibull model (see equation 1) was chosen to describe time and dose dependencies in inactivation behaviors because it has been suggested that its parameters relate with the physiological state of the bacterial population *(12, 21)*.

$$\log S(t) = \log \frac{N_t}{N_0} = -\left(\frac{t}{\alpha}\right)^{\beta} \quad (1)$$

where t is the incubation time (h), N_0 and N_t are the cell numbers at 0 h and t, and α and β are the so-called scale and shape parameters. The Weibull model (equation 1) was initially introduced to better describe changes in cell numbers after moderate thermal treatments *(34, 37)*. When using the Weibull model, deviations from the conventionally used log-linear relationship of the death time model are often observed *(26)*. The Weibull model is based on a stochastic consideration of organisms being in two distinct states, namely, "alive" or "dead," with the state changing from one to the other at a given time for an individual cell. The shape parameter (β value) is of particular significance because it corresponds to changes in the physiological conditions of cells. For example, $\beta < 1$ (upward concave) indicates that surviving cells are adapting to superimposed conditions and are, therefore, less likely to die, whereas $\beta > 1$ (downward concave) indicates that remaining cells are increasingly more susceptible to superimposed stresses *(34)*.

MATERIALS AND METHODS

Chemicals. Sodium phosphate dibasic (Na_2HPO_4) and dimethyl sulfoxide were purchased from Sigma Aldrich (Steinheim, Germany). Mueller-Hinton broth (MHB; dehydrated beef infusion at 300 g/L, casein hydrolysate at 17.5 g/L, and starch at 1.5 g/L) and Mueller-Hinton agar (MHA; dehydrated beef infusion at 300 g/L, casein hydrolysate at 17.5 g/L, starch at 1.5 g/L, and agar at 17 g/L) were obtained from Oxoid (Hampshire, UK). Standard-I nutrient broth (peptones at 15 g/L, yeast extract at 3 g/L, sodium chloride at 6 g/L, D(+)glucose at 1 g/L) was purchased from Merck (Darmstadt, Germany). Sodium chloride (NaCl) and agar-agar were obtained from Carl Roth GmbH (Karlsruhe, Germany). Potassium monobasic monohydrate ($KH_2PO_4 \cdot H_2O$) was purchased from VWR International GmbH (Darmstadt, Germany). RE1 was synthesized and purified at the Department of Food Physics and Meat Science, Institute of Food Science and Biotechnology, University of Hohenheim (Stuttgart, Germany). RE6 and RE12 were synthesized and purified at Centre de Coopération Internationale en Recherche Agronomique pour le Développement, L'Unité Mixte de Recherches Ingénierie des Agro-polymères et Technologies Émergentes (CIRAD UMR IATE; Montpellier, France). Because of the limited solubility of REs in water, each compound was dissolved in 5% dimethyl sulfoxide. The presence of 5% dimethyl sulfoxide in the stock solution did not contribute to the inhibition or inactivation of bacteria observed.

Microorganism. *S. carnosus* LTH1502 was obtained from the Department of Food Microbiology and Hygiene, Institute of Food Science and Biotechnology (University of Hohenheim). The strain was grown in MHB and on MHA. Prior to each experiment, a single colony of the culture was activated twice by incubation in MHB and was incubated at 37°C for 20 to 22 h (until the stationary phase was reached). A cell culture was prepared by centrifugation at 3,000 × *g* for 15 min at 4°C and was washed twice with phosphate-buffered saline (PBS). The cell pellets were then resuspended with either PBS or MHB to make up a final concentration of $\sim 10^8$ CFU/mL.

Macrobroth endpoint assay. To select appropriate concentrations for the scanning electron microscopy test (see below), the MBCs of RE1, RE6, and RE12 were first determined against *S. carnosus* LTH1502. An overnight culture ($\sim 10^8$ CFU/mL) of *S. carnosus* LTH1502 was collected and washed twice with PBS buffer at pH 7.2. Cultures were kept in buffer and treated without dilution with RE1, RE6, and RE12 at concentrations of up to 12.8 mM. Samples were withdrawn after 0 and 24 h of incubation at 37°C. The MBC was defined as the concentration of RE that reduced the cell number to below 10^2 CFU/mL after 24 h. For enumeration, all samples were serially diluted in 0.8% NaCl and plated on Standard-I nutrient agar using a spiral plater (Whitley Automatic Spiral Plater, Don Whitley Scientific Limited, West Yorkshire, UK). Plates were incubated at 37°C for 24 h, and colonies were counted using a colony counter (Synbiosis, Frederick, MD).

Scanning electron microscopy. Cells treated with RE1, RE6, and RE12 at the MBC (6.4, 0.2, and 0.05 mM, respectively) were examined under an SEM after 24 h of incubation at 37°C to observe changes in cell morphologies. After being treated for 24 h, cells were collected and washed twice with PBS. Pellets were redispersed in PBS, and samples of 10 μL were withdrawn and placed on membrane filters (diameter 13 mm, pore size 0.4 μm; Whatman Nuclepore Track-Etched Membranes, Sigma-Aldrich, St. Louis, MO). Filters were freeze-dried for 4 h at 2 bars and −54°C (Christ Alpha 1-2, Osterode, Germany) and were placed on aluminum stubs with double-sided carbon tape. Samples were

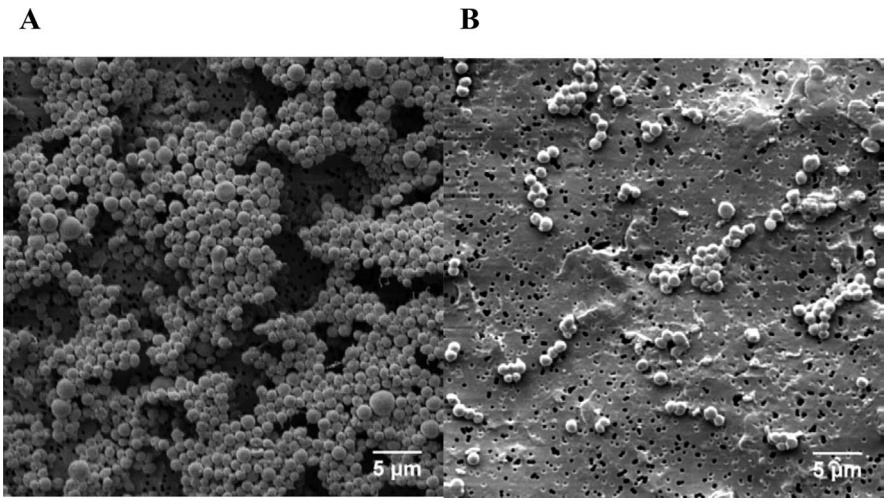

FIGURE 1. *Scanning electron microscopy images of* S. carnosus *LTH1502 cells treated with methyl rosmarinate (RE1) and hexyl rosmarinate (RE6) at the MBC and incubated at 37°C for 24 h. Images were observed at a magnification of 2,000. (A) 6.4 mM RE1 and (B) 0.2 mM RE6.*

sputter coated with gold palladium. Samples were then examined with a DSM 940 SEM (Zeiss, Oberkochen, Germany) at an accelerating voltage of 5 to 7 kV at a working distance of 8 to 9 mm.

Macrobroth time-kill assay. To obtain information about the dose-dependent behavior of the different REs, *S. carnosus* LTH1502 cells were treated with RE1, RE6 and RE12 at various ester concentrations. To that purpose, a prepared culture ($\sim 10^8$ CFU/mL) was used to inoculate MHB and was diluted to 10^4 CFU/mL. Additions of 0.2 to 6.4 mM RE1, 0.025 to 0.4 mM RE6, and 0.00625 to 0.2 mM RE12 were made to the culture, and samples were withdrawn after 0, 0.5, 1, 2, 3, 4.5, 6, 9, 12, 24, and 48 h of incubation at 37°C. MICs were defined as the concentration of ester inhibiting the growth of the culture after 48 h of incubation.

Fractional area. The overall activity of REs was assessed by determining and normalizing the area under CFU per milliliter versus time curves *(20)*. A net treatment effect was calculated by relating the area of a treated sample to that of a control (bacteria grown at 37°C without an antimicrobial agent). Henceforth, this net treatment effect will be referred to as the fractional area. Integrations and calculations were carried out using OriginPro software (version 8, OriginLab, Northampton, MA). Generally, the lower the fractional area, the more effective the treatment.

Weibull modeling. To determine the Weibull parameters, α and β (equation 1), CFU per milliliter versus time data were first normalized by division through cell numbers at $t = 0$ prior to fitting with the Weibull model. Both α and β values were then used to calculate the Weibull distribution, so-called probability density function profile f(t).

$$f(t) = \frac{\beta}{\alpha}\left(\frac{t}{\alpha}\right)^{\beta-1} \exp - \left(\frac{t}{\alpha}\right)^{\beta} \quad (2)$$

All calculations were carried out using MATLAB (version R2014b, MathWorks, Natick, MA).

Statistical analysis. All trials were carried out at least in duplicate, and measurements were made in triplicate. Means and standard errors (where needed) were calculated using Excel (Microsoft, Redmond, WA).

RESULTS

MBC and morphology of treated cells. The MBCs of *S. carnosus* LTH1502 cells treated with RE1, RE6, and RE12 were 6.4, 0.2, and 0.05 mM, respectively. The latter is in agreement with the previously published study *(32)*. Activities of REs, therefore, increased in the order of RE1 < RE6 < RE12. SEM images (Fig. 1) illustrate noticeable differences in cell morphologies after treatment with REs for 24 h. Cells treated with RE1 (Fig. 1A) were slightly swollen and clustered compared with untreated cells (not shown). Some cellular damage of *S. carnosus* LTH1502 after treatment with RE6 (Fig. 1B) is visible, with cellular fragments being present on the sputter-coated filter. Some intact cellular clusters remained that were, in appearance, similar to those treated with RE1. Complete breakdown of cellular structures and formation of large lumps of organic material were observed after treatment with RE12, which was already shown in the previous work *(33)*.

Macrobroth dilution assay. Changes in cell numbers (log CFU per milliliter) of *S. carnosus* LTH1502 over time after treatment with various concentrations of RE1, RE6, and RE12 are shown in Figure 2. From those, MICs were determined: 0.8, 0.2, and 0.05 mM for RE1, RE6, and RE12, respectively. At concentrations below the MIC, the addition of RE6 and RE12 (Fig. 2B and 2C) led to some initial decreases in cell numbers followed by rapid regrowth, whereas addition of RE1 (Fig. 2A) at concentrations below the MIC briefly delayed growth (<4 h). The initial decrease at concentrations below the MIC was less pronounced for RE6. At concentrations above the MIC, cell numbers of all treated cultures decreased over time to eventually fall below detectable levels. However, the progression of this decrease differed among the three treatments. Cells treated with RE1 appeared to remain unaffected for some time, and inactivation then occurred more rapidly at later times. In contrast, cells treated with RE6 and RE12 were immediately affected, with cell numbers rapidly decreasing after treatments. This decrease then slowed as time progressed.

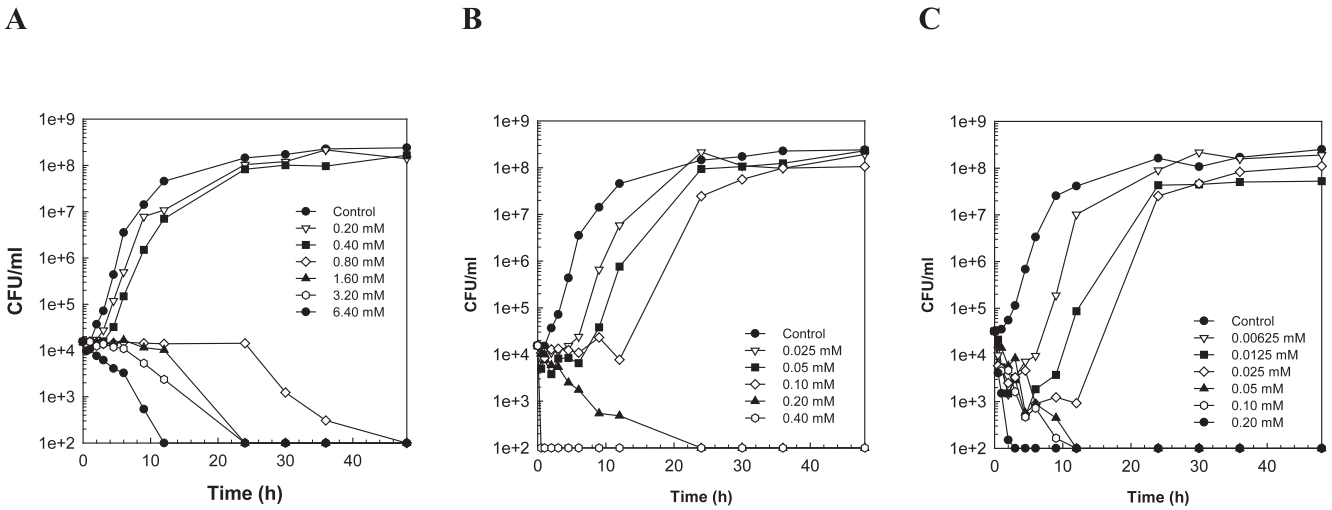

FIGURE 2. *Log CFU per milliliter versus time behavior of* S. carnosus *LTH1502 incubated at 37°C over the course of 48 h in the presence of (A) 0.2 to 6.4 mM RE1, (B) 0.025 to 0.4 mM RE6, and (C) 0.00625 to 0.2 mM RE12.*

Net effect and Weibull parameters. The log CFU per milliliter versus time data in Figure 2 at RE concentrations at and above the MIC were further analyzed by determining the fractional area (Fig. 3), the Weibull parameters α and β, and the probability function f(*t*) (Table 1 and Figs. 4 and 5).

Net effect. Figure 3 shows the net effect (normalized area under the log CFU per milliliter versus time curves) as a function of the RE concentrations used to treat *S. carnosus* LTH1502. With increasing concentrations of esters, the fractional area decreased, which indicates that the effectiveness of the treatment increased. Fractional areas for treatments with RE1 decreased little until concentrations of 0.4 mM were exceeded. In contrast, fractional areas for RE6 and RE12 decreased nearly linearly with concentration, confirming the higher effectiveness of compounds.

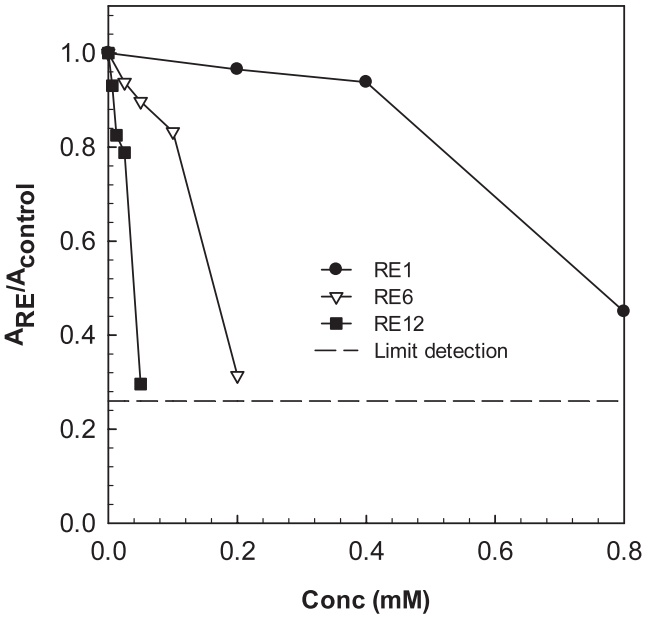

FIGURE 3. *Fractional area obtained by integration and normalization of CFU per milliliter versus time data of 10^4 CFU/mL* S. carnosus *LTH1502 cells incubated with methyl rosmarinate (RE1), hexyl rosmarinate (RE6), and dodecyl rosmarinate (RE12) at 37°C over the course of 48 h. ●, 0.2 to 0.8 mM RE1; ▽, 0.025 to 0.2 mM RE6; and ■, 0.00625 to 0.05 mM RE12.*

Weibull parameters a and β and probability function f(*t*). Table 1 shows the results of fitting survival data to the Weibull model of equation 1 to obtain the scale and shape parameters α and β. Figures 4A and 5A exemplify the compliance of the fit to the measured data for treatments with RE1, RE6, and RE12 at their respective MICs (Fig. 4A) and for treatments with RE1 at concentrations two- to eightfold higher than the MIC (Fig. 5A). Both scale and shape parameters decreased with increasing RE concentrations and with increasing alkyl chain length of esters. The shape parameter β was larger than 1 for all treatments with RE1 and smaller than 1 for all treatments with RE6 and RE12, indicating substantial differences in the shape of the inactivation curves between RE1 and RE6 and RE12. Figures 4A and 5A confirm this result, with inactivation curves of RE1 having a downward concave shape and curves of RE6- and RE12-treated cells having an upward concave shape. The calculated probability density function of equation 2 for REs at the MIC (Fig. 4B) and for RE1 at various concentrations above the MIC (Fig. 5B) indicate a substantially different development for RE1 than for RE6 and RE12. The probability function (see equation 2) represents the probability of inactivation at different treatment times. Whereas survival probabilities continuously decrease for RE6 and RE12, they initially increase and then decrease again for RE1. The surviving probability curve of cells treated with RE1 becomes short-lived when concentrations of RE1 increase, e.g., the probability density function has a maximum at 30 h of incubation at the MIC but reaches a maximum after 6 h of treatment at eight times the MIC.

TABLE 1. *Results of fitting a Weibull model to log CFU per milliliter versus time data for* S. carnosus *LTH1502 cultures incubated at 10^4 CFU/mL at 37°C for 24 h and treated with RE1, RE6, and RE12 at MIC or multiples of the MIC*[a]

Compound	Concn (mM)	Weibull parameters (95% CI) α	β	R^2	RMSE
RE1	**0.8 (MIC)**	**31.3**	**4.1**	**0.95**	**0.13**
	1.6 (2× MIC)	19.1	3.5	0.99	0.03
	3.2 (4× MIC)	14.6	1.6	0.99	0.05
	6.4 (8× MIC)	6.8	1.3	0.98	0.11
RE6	**0.2 (MIC)**	**6.6**	**0.64**	**0.98**	**0.11**
RE12	**0.05 (MIC)**	**3.2**	**0.69**	**0.93**	**0.24**
	0.1 (2× MIC)	1.5	0.44	0.95	0.19
	0.2 (4× MIC)	0.6	0.57	0.98	0.19

[a] RE1, methyl rosmarinate; RE6, hexyl rosmarinate; RE12, dodecyl rosmarinate; CI, confidence interval; RMSE, root mean squared error. MICs that were used for analysis with the Weibull model are presented in bold.

DISCUSSION

The Weibull distribution is a probability model that is based on the assumption that cells are first alive and are later inactivated due to a treatment *(26)*. There is a distribution of lethality within the treatment time. If stresses are applied, such state transitions will occur more frequently. Inactivation curve is thus a result of the time-dependent accumulation of such events *(12, 34)*. In other words, the inactivation curve is the cumulative distribution described by the Weibull model (equation 1), which can be derived from the probability function, equation 2. The Weibull model (equation 1) was previously reported to fit inactivation curves better than the log-linear model *(11)*.

Peleg and Cole *(26)* were the first to use the Weibull model to describe an inactivation process due to heating. The results indicated that *Salmonella* Typhimurium and *L. monocytogenes* were inactivated immediately after heat was applied, whereas spores of *Clostridium botulinum* and *Bacillus stearothermophilus* needed some time to be reduced in numbers. This difference in heat resistance behavior became apparent when considering the shape parameter β and could be related to the differences in bacterial cell versus bacterial spore structures. Differentiation of susceptibilities to various stresses has also been shown to be feasible by assessing β. For example, Virto and coauthors *(36)* investigated the inactivation of *Yersinia*

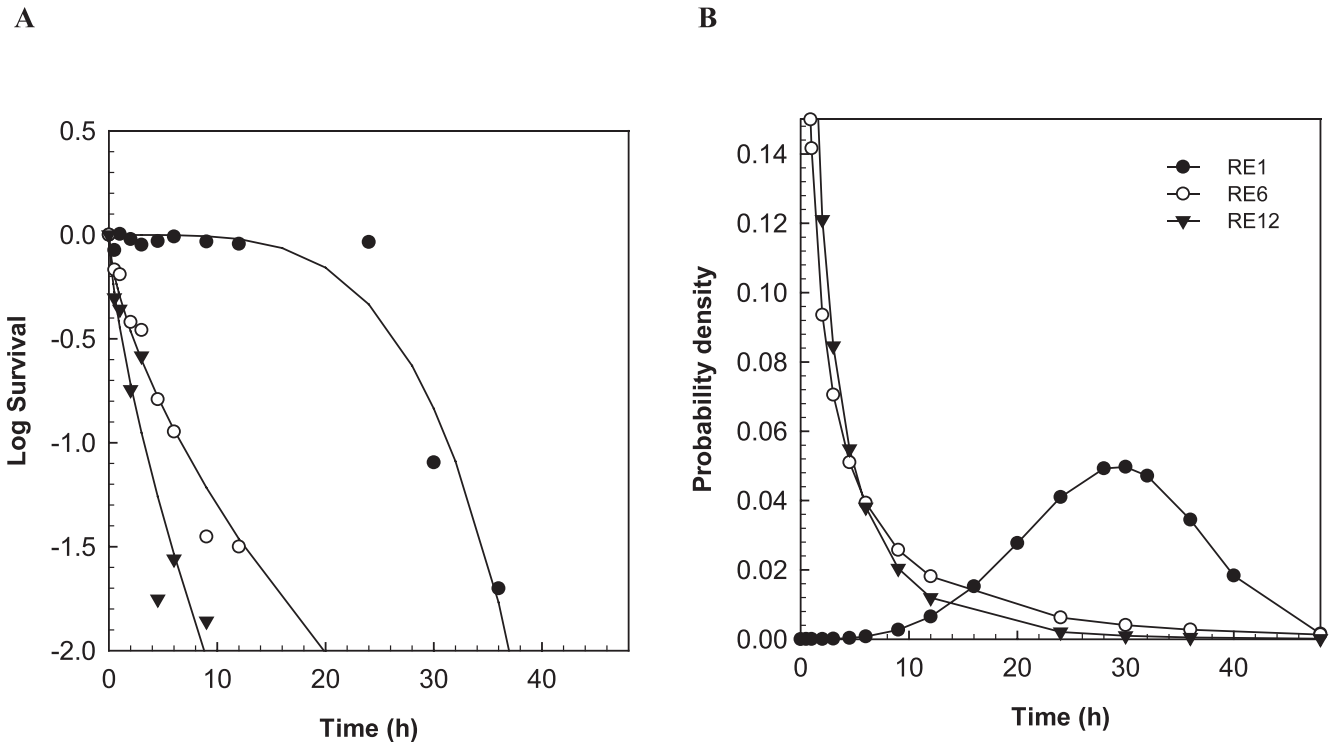

FIGURE 4. *Results of Weibull modeling of log CFU per milliliter versus time behavior of* S. carnosus *LTH1502 incubated at 37°C over the course of 48 h in the presence of methyl rosmarinate (RE1), hexyl rosmarinate (RE6), and dodecyl rosmarinate (RE12) at their MICs. (A) Fits of inactivation plot data of cultures treated with (●) 0.8 mM RE1, (○) 0.2 mM RE6, and (▼) 0.05 mM RE12. (B) Plots of the probability density function of cells treated with (●) 0.8 mM RE1, (○) 0.2 mM RE6, and (▼) 0.05 mM RE12.*

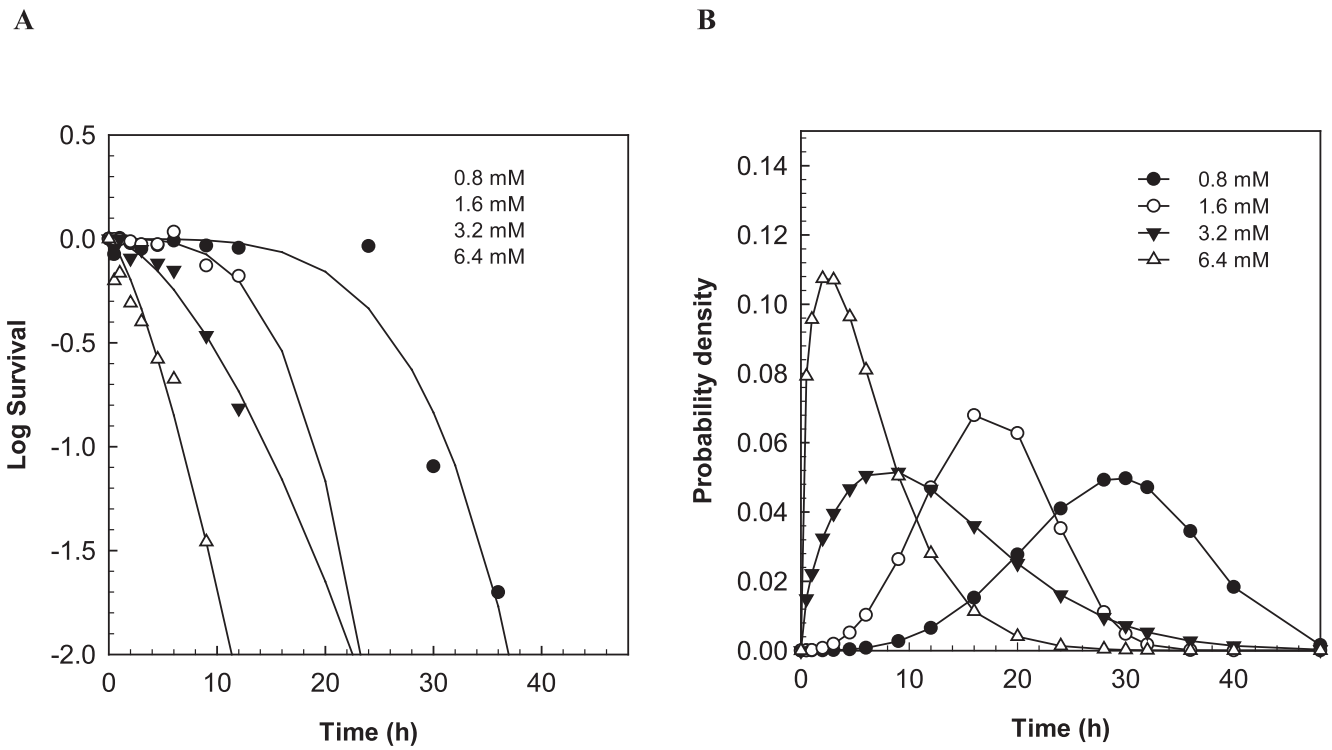

FIGURE 5. *Results of Weibull modeling of log CFU per milliliter versus time behavior of* S. carnosus *LTH1502 incubated at 37°C over the course of 48 h in the presence of methyl rosmarinate (RE1), at concentrations ranging from 0.8 to 6.4 mM. (A) Fits of inactivation plot data. (B) Plots of the probability density function.*

enterocolitica by citric and lactic acids at different temperatures. Results of their Weibull modeling indicated that the β value depended on the type of acid and temperature but not on the concentration of acid *(36)*. From this, they concluded that protonation state and ability of organic acids to pass through membranes was affected by temperature and that lactic acid was generally more lethal than citric acid at any concentration and pH value of organic acid. As such, one may gain an insight into mechanistic actions through application of nonlinear models.

The Weibull model has been used in this study to allow for a differentiation in the effect of a treatment with antimicrobials that have systematic variations in the nature of their chemical structures. Results show a critical change in the effect of an antimicrobial agent upon esterification of rosmarinic acid with aliphatic alkyl alcohols having chain lengths $\geq$6. This correlates well with observed changes in cell morphologies after treatment with REs by electron microscopy. One can observe a transition of the shape parameter β from being larger than 1 to being smaller than 1 upon esterification with alcohols having larger chains lengths. This is also manifested in changes in the progression of the probability density with time. Apparently, the treatment of cells with RE1 does not immediately cause damage to cells; rather the compound requires some incubation time to begin to work. In contrast, addition of RE6 and RE12 has an immediate effect and the probability density declines continuously after treatment. This suggests that the mode of action of compounds changes.

Lipophilization has previously been shown to change the mode of action of a variety of compounds *(15)*. Grafting of a lipophilic moiety to compounds such as sugars, amino acids, proteins, or phenolic compounds can be achieved by chemical or enzymatic means *(35)*. For example, the esterification of chlorogenic acid with alcohols yielded butyl and octyl esters that had equal free radical scavenging activity in menhaden oil-in-water emulsions as free chlorogenic acid, whereas antioxidant activity of the dodecyl ester was completely lost *(30)*. This was attributed to changes in the location of compounds due to alterations in their physical properties. Specifically, surface activity and partitioning in the lipid phase of emulsions increased with increasing length of the alkyl chain. When the antioxidant activity of caffeic acid esterified with alcohols in mayonnaise and milk with added fish oil was assessed, authors reported that esters with medium alkyl chain length improved the oxidative stability of mayonnaise better than esters with a methyl or octadecyl tail *(2)*. In milk, though, caffeates were short alkyl chains that were more active than medium and long chains. Recently, branched alkyl ferulates were found to be highly effective in inhibiting oxidation of fish oil–enriched milk *(2)*. Methyl ferulate followed by ferulic acid and butyl ferulate were the most effective, whereas octyl ferulate was prooxidative. This complete reversal of functionality was found to become more pronounced at alkyl chain lengths of C8 to C12.

Changes in localization of compounds and affinity to surfaces were found to be key contributors to the above-mentioned results. Generally, lipophilized hydrophilic agents including rosmarinic acid become more surface active upon esterification. As for antimicrobial activity, however, the results of this study indicate that these

TABLE 2. *Relationship between the log of 1/α and the concentration of RE1 and RE12*[a]

Compound	Avg β value	Equation	R^2
RE1	2.6	Log (1/α) = 0.09[RE1] − 1.485	0.91
RE12	0.57	Log (1/α) = 4.2[RE12] − 0.6826	0.97

[a] RE1, methyl rosmarinate; RE12, dodecyl rosmarinate. The α value was obtained by fitting a Weibull model to log CFU per milliliter versus time data for *S. carnosus* LTH1502 cultures incubated at 10^4 CFU/mL at 37°C for 24 h with average β value.

physicochemical properties must change to a certain extent to alter their mode of action. Apparently, the increase in surface activity in RE1 is insufficient to cause a substantially enhanced association with bacterial membranes. Possibly, the molecule is also still small enough to be transported through the cell membranes. In mode of action, therefore, it continues to function just like rosmarinic acid. In contrast, RE6 and RE12 have a sufficiently enhanced affinity for cell membranes and, therefore, are able to disrupt them. This lowers the concentrations required to inactivate cells and also causes them to have a more immediate effect, possibly because there is no barrier to diffusion. There is, rather, adsorption from the surrounding aqueous phase.

Upward concavity in inactivation curves has been found to be characteristic of other compounds that cause cell membrane damage. For example, the applications of copper against *Staphylococcus haemolyticus (8),* tea tree oil against *S. aureus (4),* daptomycin against *S. aureus (29),* and chitosan against *E. coli* and *S. aureus (5)* have all yielded upward concave survival curves. In contrast, application of vancomycin, an inhibitor of peptidoglycan synthesis of cells, yielded downward concave survival curves *(3, 9, 17)*. The different concavities of the inactivation curves also correspond to distinguishable probability density functions. The upward concave curve yields no-peak (tailing) probability density function, which shows the survival of resistance cells and the rapid reduction of sensitive cells. The long tail indicates a resistant population *(25)*. The existence of resistant populations could implicate the regrowth pattern of RE6 and RE12 treatment at lower MICs. In contrast, the downward concave curve yields a bell-shaped curve of probability density function, which indicates that the population was injured with the onset of inactivation *(25)*. This could implicate the long inactivation shoulder of RE1 treatment.

The results of this study indicate that the scale parameter (α value) decreased as the concentrations of RE1 and RE12 increased above the MIC. The concentration of the antimicrobial agent mainly influenced the α value, which implies the inactivation rate. The similar effectiveness of citric acid and lactic acid against *Y. enterocolitica* was shown *(36)*. The higher the acid concentration, the smaller the α value and the faster the inactivation. However, it would be inappropriate to state directly that the scale parameter represents dosage of the antimicrobial agent. This is because the α value correlates strongly to the shape parameter (β value) *(19)*. The relationship between 1/α and the concentration of the antimicrobial agent by fixing the β value can be presented, instead. The β value of RE1 and RE12 treatments were set at their average values (2.6 and 0.57, respectively), and their survival curves were refitted into equation 1 to obtain the α values. Then, the log of 1/α of each RE6 and RE12 were plotted against their concentrations to describe the relationship (Table 2). The relationships between the log of 1/α and the concentrations of RE1 and RE12 are linear, which describes the proportion of concentration to inactivation time. The greater slope of RE12 equations also indicates that the inactivation time of RE12 depends more on the concentration than is the case with RE1.

In conclusion, results of this study showed that application of nonlinear modeling of time-kill curves combined with electron microscopy can yield additional insights into changes that occur upon altering the chemical structure of naturally occurring antimicrobials (here rosmarinic acid) via esterification. A critical chain length of alkyl alcohols is required for them to act on membranes rather than intracellularly. Corresponding to these changes in the mode of action, compounds may work more rapidly or exhibit time delays in their action, as shown by an analysis of parameters obtained by nonlinear modeling. The data from parameters can be used to implement antimicrobial application. As a next step, studies should be conducted with varying microbial populations to assess how this transitioning from an intracellular mode of action to a membrane mode depends on the nature of the microbial envelope. Moreover, the effect of addition of solubilizing agents, cosolvents, or chelators that could all change mass transport and partitioning of antimicrobials should be studied.

ACKNOWLEDGMENTS

This project was supported by funds from the University of Hohenheim Experiment Station and by a dissertation completion grant of the DAAD program "STIBET Doktoranden." We sincerely appreciate the intriguing discussions with Prof. Dr. Micha Peleg of the University of Massachusetts with respect to the use of appropriate mathematical kinetic growth models.

REFERENCES

1. Abedini, A., V. Roumy, S. Mahieux, M. Biabiany, A. Standaert-Vitse, C. Rivière, S. Sahpaz, F. Bailleul, C. Neut, and T. Hennebelle. 2013. Rosmarinic acid and its methyl ester as antimicrobial components of the hydromethanolic extract of *Hyptis atrorubens* Poit. (Lamiaceae). *Evid. Based Complement. Alternat. Med.* 2013:1–11. doi:10.1155/2013/604536.
2. Alemán, M., R. Bou, F. Guardiola, E. Durand, P. Villeneuve, C. Jacobsen, and A.-D. M. Sørensen. 2015. Antioxidative effect of lipophilized caffeic acid in fish oil enriched mayonnaise and milk. *Food Chem.* 167:236–244. doi:10.1016/j.foodchem.2014.06.083.
3. Brauers, J., M. Kresken, A. Menke, A. Orland, and I. Morrissey. 2006. Evaluation of daptomycin, vancomycin, teicoplanin and linezolid against *Staphylococcus aureus, Enterococcus faecalis* and *Enterococcus faecium* utilising in vitro time-kill methodology, p. 1583. 16th European Congress of Clinical Microbiology and Infectious Diseases, Nice, France, 1 to 4 April 2006.

4. Campion, J. J., P. J. McNamara, and M. E. Evans. 2005. Pharmacodynamic modeling of ciprofloxacin resistance in *Staphylococcus aureus*. *Antimicrob. Agents Chemother*. 49:209–219. doi:10.1128/aac.49.1.209-219.2005.
5. Carson, C. F., B. J. Mee, and T. V. Riley. 2002. Mechanism of action of *Melaleuca alternifolia* (tea tree) oil on *Staphylococcus aureus* determined by time-kill, lysis, leakage, and salt tolerance assays and electron microscopy. *Antimicrob. Agents Chemother*. 46:1914–1920. doi:10.1128/aac.46.6.1914-1920.2002.
6. Cuvelier, M.-E., H. Richard, and C. Berset. 1996. Antioxidative activity and phenolic composition of pilot-plant and commercial extracts of sage and rosemary. *J. Am. Oil Chem. Soc*. 73:645–652. doi:10.1007/bf02518121.
7. Davidson, P. M., J. N. Sofos, and A. L. Branen. 2005. Antimicrobials in food. CRC Press, Boca Raton, FL.
8. Drusano, G. L., A. Louie, M. Deziel, and T. Gumbo. 2006. The crisis of resistance: identifying drug exposures to suppress amplification of resistant mutant subpopulations. *Clin. Infect. Dis*. 42:525–532. doi:10.1086/499046.
9. Flandrois, J. P., G. Fardel, and G. Carret. 1988. Early stages of in vitro killing curve of LY146032 and vancomycin for *Staphylococcus aureus*. *Antimicrob. Agents Chemother*. 32:454–457. doi:10.1128/aac.32.4.454.
10. Ganewatta, M. S., and C. Tang. 2015. Controlling macromolecular structures towards effective antimicrobial polymers. *Polymer* 63:A1–A29. doi:10.1016/j.polymer.2015.03.007.
11. González, M., and M. L. Hänninen. 2012. Effect of temperature and antimicrobial resistance on survival of *Campylobacter jejuni* in well water: application of the Weibull model. *J. Appl. Microbiol*. 113:284–293. doi:10.1111/j.1365-2672.2012.05342.x.
12. Horowitz, J., M. D. Normand, M. G. Corradini, and M. Peleg. 2010. Probabilistic model of microbial cell growth, division, and mortality. *Appl. Environ. Microbiol*. 76:230–242. doi:10.1128/aem.01527-09.
13. Jordán, M. J., V. Lax, M. C. Rota, S. Lorán, and J. A. Sotomayor. 2012. Relevance of carnosic acid, carnosol, and rosmarinic acid concentrations in the in vitro antioxidant and antimicrobial activities of *Rosmarinus officinalis* (L.) methanolic extracts. *J. Agr. Food Chem*. 60:9603–9608. doi:10.1021/jf302881t.
14. Jung, Y., and K. R. Matthews. 2015. Development and application of novel antimicrobials in food and food processing, p. 347–364. *In* C.-Y. Chen, X. Yan, and C. R. Jackson (ed.), Antimicrobial resistance and food safety. Academic Press, San Diego, CA.
15. Laguerre, M., C. Bayrasy, J. Lecomte, B. Chabi, E. A. Decker, C. Wrutniak-Cabello, G. Cabello, and P. Villeneuve. 2013. How to boost antioxidants by lipophilization? *Biochimie* 95:20–26. doi:10.1016/j.biochi.2012.07.018.
16. Li, X., X. Shi, M. Wang, and Y. Du. 2011. Xylan chitosan conjugate—a potential food preservative. *Food Chem*. 126:520–525. doi:10.1016/j.foodchem.2010.11.037.
17. Liu, H., Y. Du, X. Wang, and L. Sun. 2004. Chitosan kills bacteria through cell membrane damage. *Int. J. Food Microbiol*. 95:147–155. doi:10.1016/j.ijfoodmicro.2004.01.022.
18. Lu, Y., and L. Y. Foo. 1999. Rosmarinic acid derivatives from *Salvia officinalis*. *Phytochemistry* 51:91–94.
19. Mafart, P., O. Couvert, S. Gaillard, and I. Leguerinel. 2002. On calculating sterility in thermal preservation methods: application of the Weibull frequency distribution model. *Int. J. Food Microbiol*. 72:107–113. doi:10.1016/S0168-1605(01)00624-9.
20. Manrique, Y., S. Suriyarak, M. Gibis, H. Schmidt, and J. Weiss. 2016. Survival of spoilage bacteria subjected to sequential eugenol and temperature treatments. *Food Microbiol*. 218:6–16. doi:10.1016/j.ijfoodmicro.2015.10.027.
21. McKellar, R. C., and X. Lu. 2004. Primary models. *In* R. C. McKellar and X. Lu (ed.), Modeling microbial responses in food. CRC Press, Boca Raton, FL.
22. Metlay, J. P., J. H. Powers, M. N. Dudley, K. Christiansen, and R. G. Finch. 2006. Antimicrobial drug resistance, regulation, and research. *Emerg. Infect. Dis*. 12:183–190. doi:10.3201/eid1202.050078.
23. Min, K. Y., H. J. Kim, K. A. Lee, K.-T. Kim, and H.-D. Paik. 2014. Antimicrobial activity of acid-hydrolyzed *Citrus unshiu* peel extract in milk. *J. Dairy Sci*. 97:1955–1960. doi:10.3168/jds.2013-7390.
24. Moreno, S., T. Scheyer, C. S. Romano, and A. A. Vojnov. 2006. Antioxidant and antimicrobial activities of rosemary extracts linked to their polyphenol composition. *Free Radic. Res*. 40:223–231. doi:10.1080/10715760500473834.
25. Peleg, M. 2006. Isothermal microbial heat inactivation, p. 11–26. *In* F. M. Clydesdale (ed.), Advanced quantitative microbiology for foods and biosystems: models for predicting growth and inactivation. CRC Press, Boca Raton, FL.
26. Peleg, M., and M. B. Cole. 1998. Reinterpretation of microbial survival curves. *Crit. Rev. Food Sci. Nutr*. 38:353–380. doi:10.1080/10408699891274246.
27. Petersen, M. S. 1991. Characterization of rosmarinic acid synthase from cell cultures of *Coleus blumei*. *Phytochemistry* 30:2877–2881.
28. Razzaque, A., and B. E. Ellis. 1977. Rosmarinic acid production in *Coleus* cell cultures. *Planta* 137:287–291. doi:10.1007/bf00388164.
29. Santo, C. E., D. Quaranta, and G. Grass. 2012. Antimicrobial metallic copper surfaces kill *Staphylococcus haemolyticus* via membrane damage. *Microbiologyopen* 1:46–52. doi:10.1002/mbo3.2.
30. Sasaki, K., J. Alamed, J. Weiss, P. Villeneuve, L. J. López Giraldo, J. Lecomte, M.-C. Figueroa-Espinoza, and E. A. Decker. 2010. Relationship between the physical properties of chlorogenic acid esters and their ability to inhibit lipid oxidation in oil-in-water emulsions. *Food Chem*. 118:830–835. doi:10.1016/j.foodchem.2009.05.070.
31. Spellberg, B., J. H. Powers, E. P. Brass, L. G. Miller, and J. E. Edwards. 2004. Trends in antimicrobial drug development: implications for the future. *Clin. Infect. Dis*. 38:1279–1286. doi:10.1086/420937.
32. Suriyarak, S., C. Bayrasy, H. Schmidt, P. Villeneuve, and J. Weiss. 2013. Impact of fatty acid chain length of rosmarinate esters on their antimicrobial activity against *Staphylococcus carnosus* LTH1502 and *Escherichia coli* K-12 LTH4263. *J. Food Prot*. 76:1539–1548. doi:10.4315/0362-028X.JFP-12-254.
33. Suriyarak, S., M. Gibis, H. Schmidt, P. Villeneuve, and J. Weiss. 2014. Antimicrobial mechanism and activity of dodecyl rosmarinate against *Staphylococcus carnosus* LTH1502 as influenced by addition of salt and change in pH. *J. Food Prot*. 77:444–452. doi:10.4315/0362-028X.JFP-13-239.
34. van Boekel, M. A. J. S. 2002. On the use of the Weibull model to describe thermal inactivation of microbial vegetative cells. *Int. J. Food Microbiol*. 74:139–159. doi:10.1016/S0168-1605(01)00742-5.
35. Villeneuve, P. 2007. Lipases in lipophilization reactions. *Biotechnol. Adv*. 25:515–536. doi:10.1016/j.biotechadv.2007.06.001.
36. Virto, R., D. Sanz, I. Álvarez, Condón, and J. Raso. 2005. Inactivation kinetics of *Yersinia enterocolitica* by citric and lactic acid at different temperatures. *Int. J. Food Microbiol*. 103:251–257. doi:10.1016/j.ijfoodmicro.2004.11.036.
37. Virto, R., D. Sanz, I. Álvarez, S. Condón, and J. Raso. 2006. Application of the Weibull model to describe inactivation of *Listeria monocytogenes* and *Escherichia coli* by citric and lactic acid at different temperatures. *J. Sci. Food Agric*. 86:865–870. doi:10.1002/jsfa.2424.